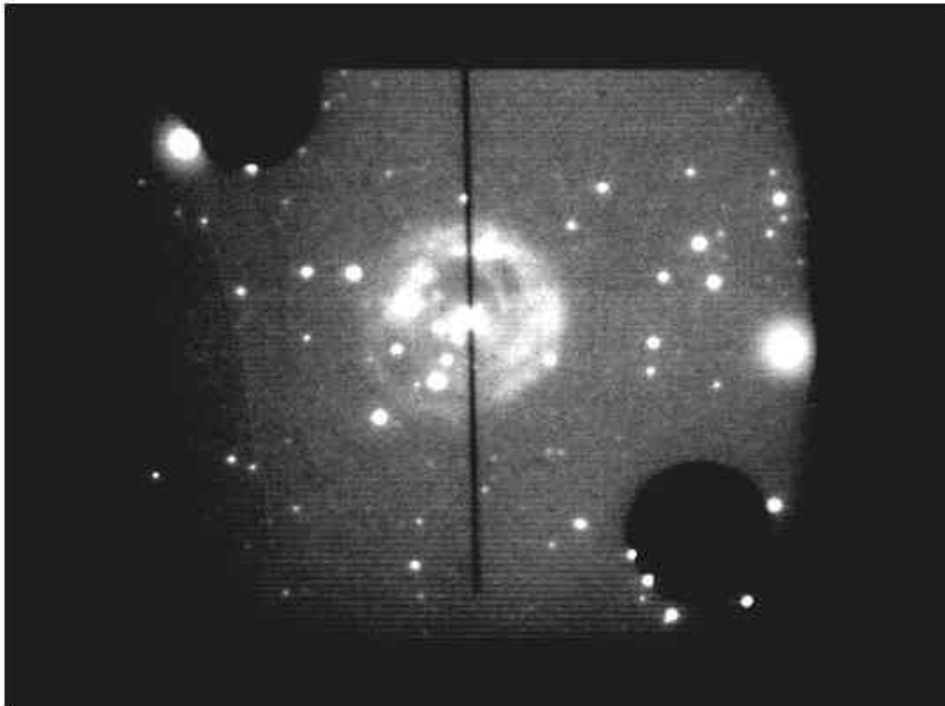# BIMONTHLY SUMMARY

September - October 2002

An image of the Blue Channel slit plate, captured from the guider camera. The object on the 2 arcsec slit is the symbiotic star V838 Mon. The apparent nebulosity surrounding the star is the light echo from a recent outburst. Image by T. Pickering.

Personnel

G. Grant Williams started his position as the Firestone Postdoctoral Fellow on September 1. Grant comes to the MMTO from Steward where he worked on the 90-Prime imager project.

Dan Blanco accepted the position of Assistant Director for Operations and will start mid November. He was the MMTO Mechanical Engineer 1983-1990. In fact, many of the features of the 6.5 m telescope (such as the inverted Serrurier truss) are a direct result of Dan's work. Dan left the

MMTO to join the WIYN project on Kitt Peak where he worked on the thermal control system and the optimization of the telescope's performance. From WIYN he went to EOS Technologies, a firm that has produced a number of modern technology telescopes including the Keck outriggers. Dan brings a wealth of experience in telescope design and optimization to the MMTO. We are sure that his contribution will be significant and quickly-felt.

C. Foltz participated in FLWO's volunteer recognition night October 29. Among the other astronomers who discussed the various projects on Mt. Hopkins were A. Szentgyorgyi, W. Traub, and E. Falco. D. Brocious and K. Erdman-Myres coordinated the event which was, as usual, very well attended.

Development

Primary Mirror Thermal Control System

In September a new heat exchanger assembly was installed in the pit to add additional cold weather capacity for the primary mirror support ventilation system. This system was designed and assembled by the MMT mechanical team of S. Callahan, R. James, and C. O'Neal with drafting support from S. Bauman, C. Wainwright, and C. Chute. P. Spencer designed the thermocouples system and valve control. The computer interface to read the thermocouples and to control the valves was made by D. Gibson. Welding support during the installation was provided by P. Ritz.

Ron James (foreground) and Clede O'Neal during final installation of the pit heat exchanger.

An issue of concern has been the performance monitoring and modification of the system's heat exchangers. The present system uses two implementations of type T thermocouples. The first is a solid wire jacketed type installed into a thermowell placed in the heat exchanger air stream. The

second type uses very fine wire attached to a flat, flexible self-adhesive pad that is mounted on the surface of the input/output fluid pipes to the heat exchanger. The thermocouples are direct wired to a DAU, which is then fed into the Cyclades via the RS232 link.

To improve temperature-monitoring accuracy, a thermocouple calibration scheme is being developed. P. Spencer configured a portable calibration chamber composed of an off-the-shelf CPU thermal electric cooler (Peltier TC array) with an attached fan, and a chunk of 2" thick Styrofoam with an excavated area to form a thermowell chamber. Another piece of Styrofoam is fitted to the thermowell chamber for sealing and maintaining fixed position for two thermocouples placed inside the calibration apparatus. Two thermocouples are placed in the chamber, one of which is designated the reference. The thermal electric cooler is then connected to a DC voltage power source to cool the chamber and maintain a constant temperature. The two thermocouples' temperatures are then measured and compared using a DAU. The difference in temperature between the two thermocouples can be used as a first-order offset value for calibration. (When the thermocouples are compared over several different temperatures, a slope and an offset can be observed for producing calibration curves.) The calibration chamber was then brought to the pit heat exchanger and used to calibrate the five thermocouples measuring heat exchanger air stream temperatures using thermocouple #1 as the reference. From this, four temperature offsets were generated. These offsets were applied to temperature readings from the air thermocouples. This first-order calibration is presently in the process of being evaluated.

A total of five new GUIs were developed for controlling and monitoring the thermal system. These GUIs use the new data server (see below) to query the current thermal system values and to control thermal system components, such as the Carrier and Neslab chillers. The GUIs include: 1) an overall thermal status summary, 2) details of the shop thermal components, 3) details of the pit thermal components, 4) details of lateral variable of the front plate, mid plate, and back plate for the primary mirror, and 5) 24-hour plots of up to 18 thermal system parameters. These GUIs interact with the XML-style data server logs.

Mount Servos

The elevation tape encoders were installed and the encoder heads aligned using a Heidenhain alignment tool borrowed from LBTO. The west encoder head was installed and connected to the elevation servo control LM628 through the existing 25X interpolator previously used for the west motor shaft encoder. The east unit was installed and pre-aligned, but the alignment proved to be difficult due to the head mount being bent during a previous motor removal operation. As of now, the east unit provides good counting mark signals, but somewhat unreliable index mark detection. We await installation of additional shims to complete the alignment to the level of accuracy achieved by the west head.

The elevation servo loop was then closed around the west tape head and the servo was re-tuned. The servo behavior appears to be much improved when tracking with wind buffeting, though not yet as stiff as required. SAO has agreed to provide some consultant help on improving the servo system, an offer we will pursue during the next reporting period.

Tracking Performance

Now that the guider logs are being archived on a nightly basis, it is possible to use them to profile the tracking performance of the telescope. A good example of performance in good conditions is shown in Figure 1 where the telescope is tracking an object setting in the west with light winds. In this case the rms of the position errors calculated by the guider is about 0.06" with a peak-to-peak error of about 0.1". [Note that these errors include a component due to the error in computing the image's centroid. This varies with the guide star's brightness and the seeing. Under good conditions, the centroiding errors are typically about 0.04" rms.] Under windier conditions, things are not quite as good as shown in Figure 1 where the winds were largely out of the east at about 25-30 mph with the telescope pointed directly into the wind after about 10:45 UT that night. Here the rms tracking error is 0.2-0.3" with peak-to-peak of up to 1.5" under the highest wind loading. This is qualitatively better than it was before the installation of the absolute tape encoders on the elevation drive arcs, but there is still room for improvement.

Of greater concern are the systematic errors visible in Figure 1. This is seen most strikingly when the cumulative tracking is plotted as in Figure 2. There is very obvious cyclical behavior in both elevation and azimuth, with a nearly constant frequency in elevation and a frequency that decreases over time in azimuth. These data were taken while tracking an object that was setting in the west with an elevation velocity that was nearly constant, and an azimuth velocity that was decreasing to near zero by the end of the observation. Figure 3 is another example where an object is tracked as it crossed the meridian. It clearly shows that the elevation frequency decreases before and then increases after the meridian crossing, while the azimuth frequency remains high and relatively constant as the telescope swings around from east to west. Figure 4 is an example where the elevation and azimuth velocities are nearly equal and constant, which allows a more direct comparison of periods and amplitudes. While the guider does a good job of correcting for these oscillations while it's running, the 0.5-1.0" amplitude is currently the largest source of pointing error as judged by the 1" rms of the latest pointing run. What's worse, it means that even offsetting from a known good position cannot really be trusted to better than 1.5-2.0". This has been noted by some observers who have tried to do blind offsetting, though others have not reported problems.

The variation of the frequency of the oscillations with tracking velocity points to the cause of the problem being spatially constant. The spatial period is also suspiciously close to 1024 cycles/rev that is an integer harmonic of the 512 cycles/rev natural frequency of the Inductosyn absolute encoders. To help test this further, T. Trebisky developed a small tool that logs the output from the Inductosyn absolute encoders (one each for azimuth and elevation) as well as the absolute tape encoders on the elevation drive arcs. This tool was then run while the telescope was commanded to move at a constant velocity. The results of the first of these tests are shown in Figure 5 where the telescope was moving at a constant 0.004 degrees/sec. In this case, the velocity was applied by commanding the inner servo loop while keeping the outer loop open. This results in a fair amount of aperiodic, mechanical noise in the position readouts of the encoders. In Figure 5 this is best seen in the "Tape 1 - Tape 2" panel. Only Tape 2 has been fully calibrated so the output of Tape 1 differs by a constant factor. Subtracting the mechanical signal as measured by Tape 2 from the absolute encoder readouts results in a very obvious sinusoidal signal with an almost 0.4" amplitude and a 1024 cycles/rev frequency (about 85 seconds), similar to what has been seen on the sky.

Clearly, there is something strange going on that affects both axes in a similar way. D. Clark did some tuning of the electronics for the elevation Inductosyn encoder and performed additional

constant velocity tests. He found that the amplitude of the 1024 cycles/rev oscillation changed with position of the telescope, but was not affected noticeably by the tuning. Subsequent guider data taken after the tuning also showed little to no change. More tests were done with all of the raw Inductosyn encoder data read out and saved at the full data rate. There were no visible artifacts in the indexer and resolver data that would suggest a stuck bit or anything to that effect. Running a similar test, but with the outer servo loop closed, does show the improvement to the elevation encoder, however (Figure 6). The rms noise in elevation is down to a few tens of milliarcsec. The azimuth electronics were not tuned so there are still some artifacts there. The 1024 cycles/rev oscillation is not seen in the outer loop test because the outer loop uses the Inductosyn encoders as the position references. A new test with the outer loop closed needs to be done where the tape encoders are read out to provide an independent measure of position. If the 1024 cycles/rev oscillation is seen in the tape encoder outputs in that test, that would fully confirm that the underlying problem indeed rests in the Inductosyn. What exactly the problem could be is still a mystery.
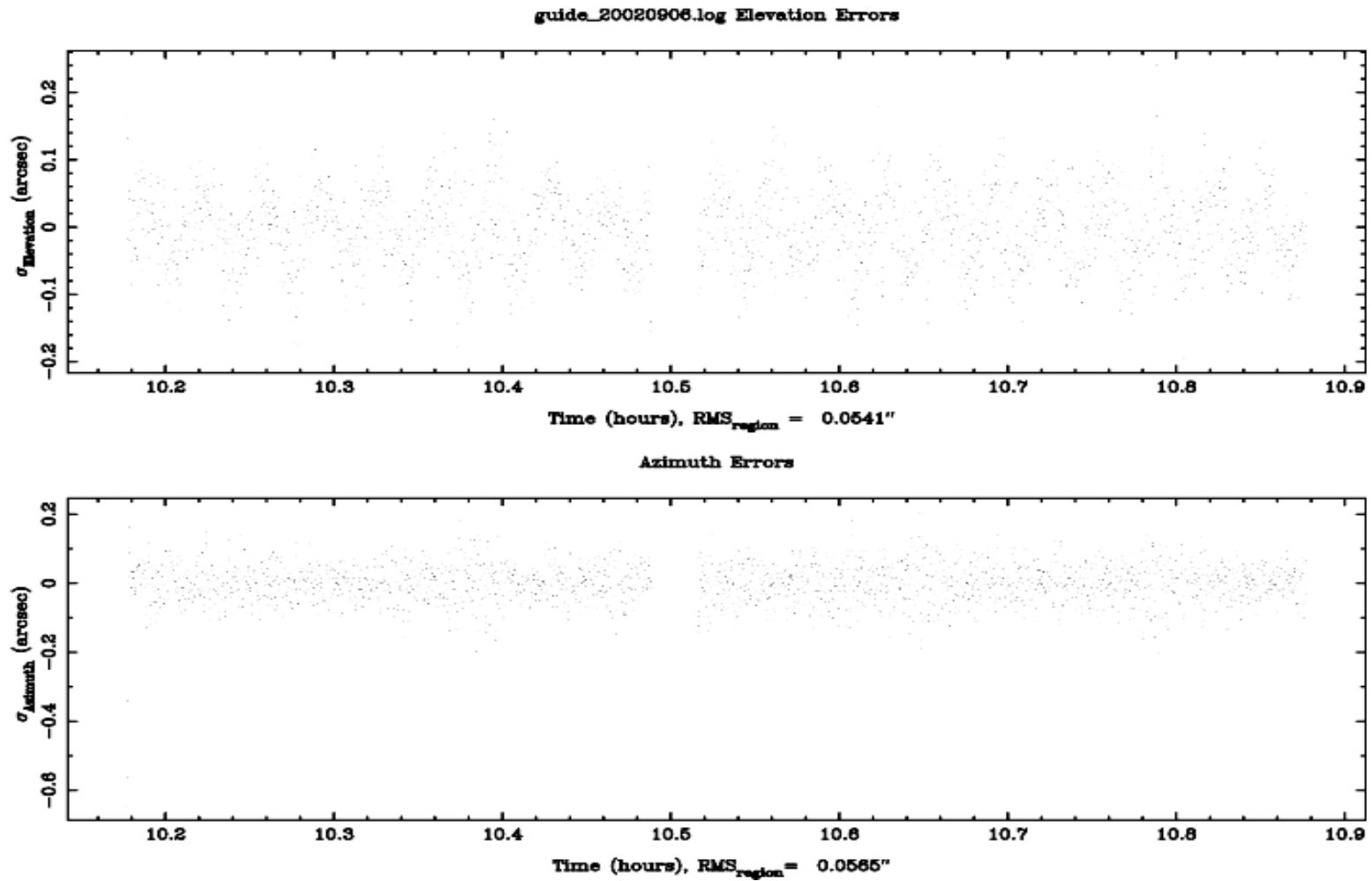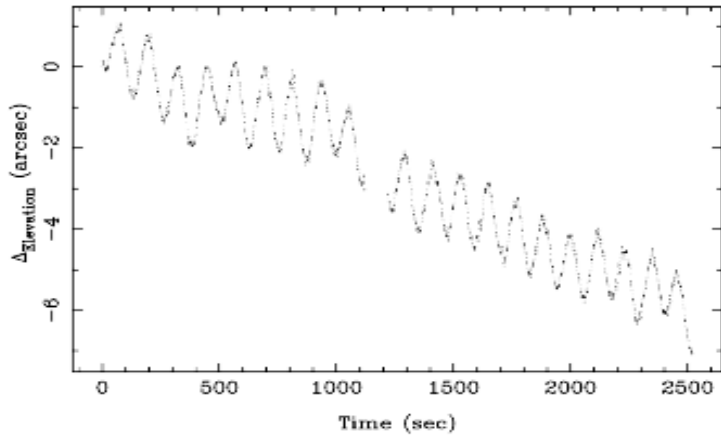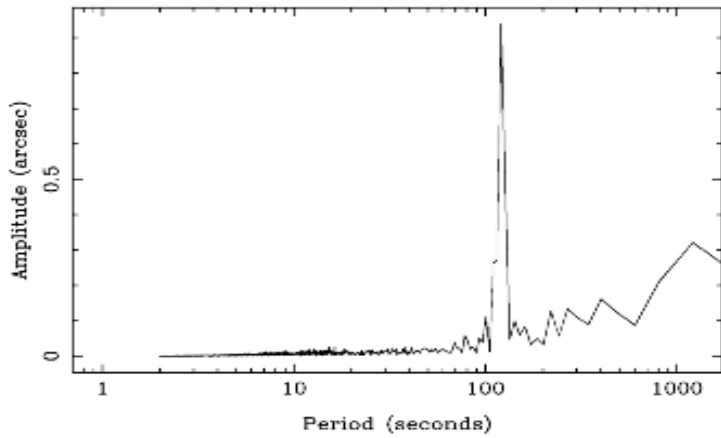
Figure 1: Raw tracking errors for the night of September 6, 2002. The raw errors are the actual differences between the reference position and the measured positions. These are multiplied by the guider's gain parameter (usually 0.5) to calculate the correction to send to the mount.
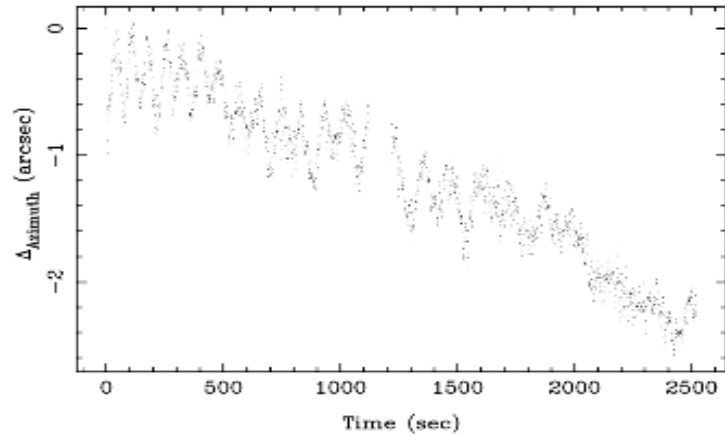
Cumulative Raw Elevation Errors between 10:10:37 and 10:52:38

Cumulative Raw Azimuth Errors between 10:10:37 and 10:52:38

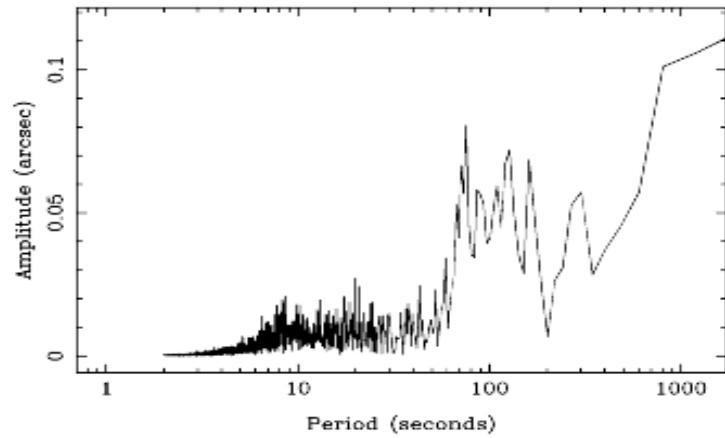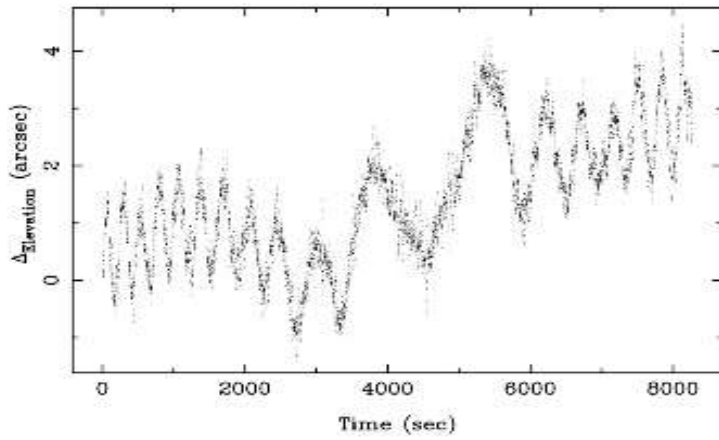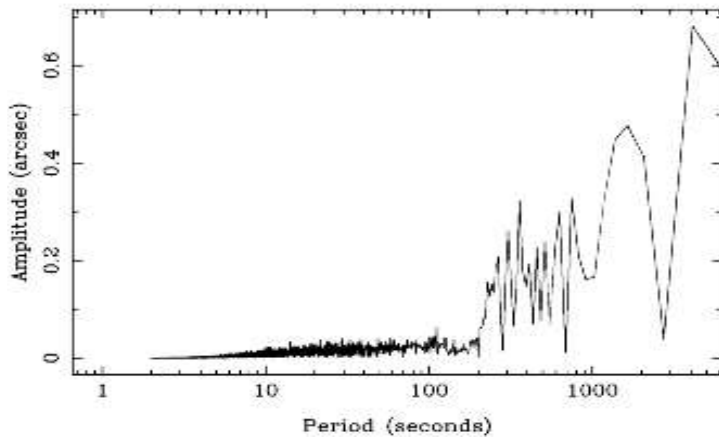Elevation FFT

Azimuth FFT

Figure 2: Cumulative tracking performance for the night of September 6, 2002. This is calculated by cumulatively summing the raw tracking errors which results in a measure of how the telescope has tracked over time.
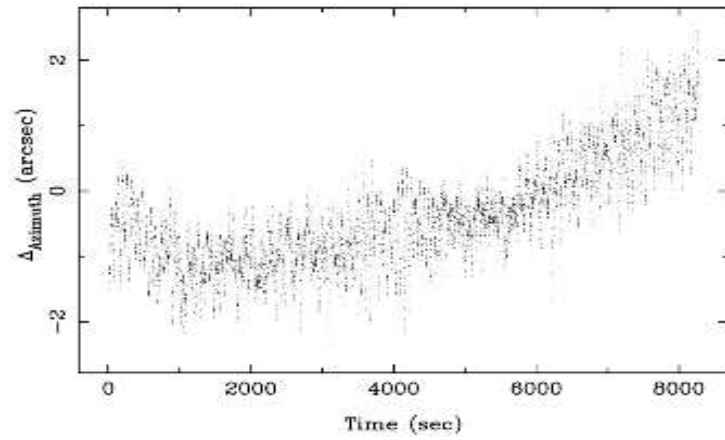
Cumulative Raw Elevation Errors between 06:53:49 and 09:11:46

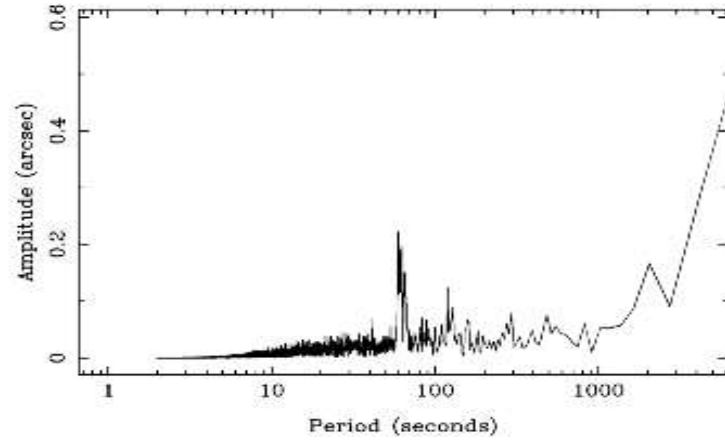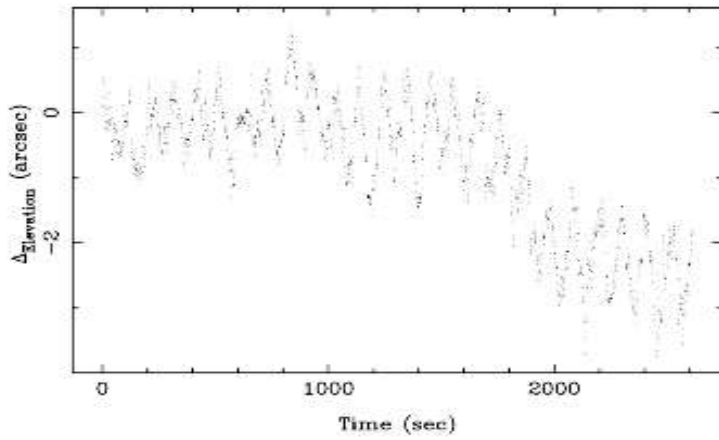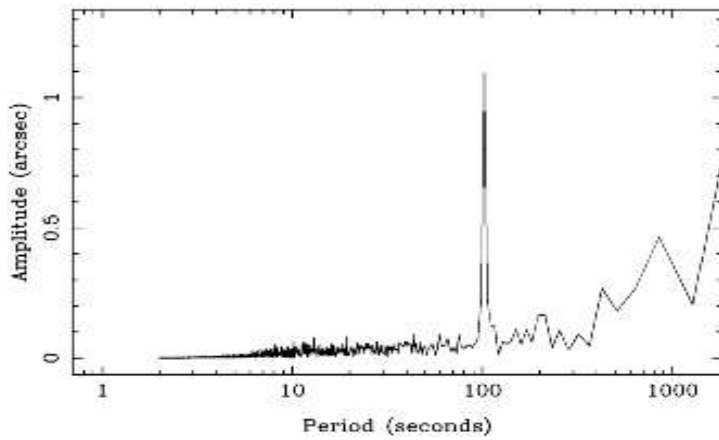Cumulative Raw Azimuth Errors between 06:53:49 and 09:11:46

Elevation FFT

Azimuth FFT

Figure 3: Tracking performance while observing an object as it crossed the meridian.
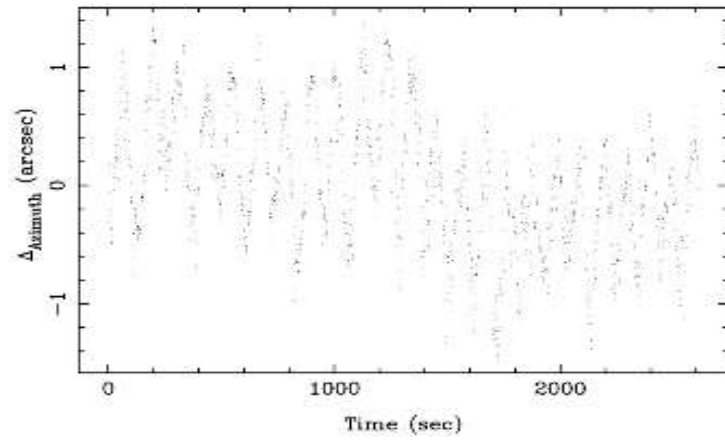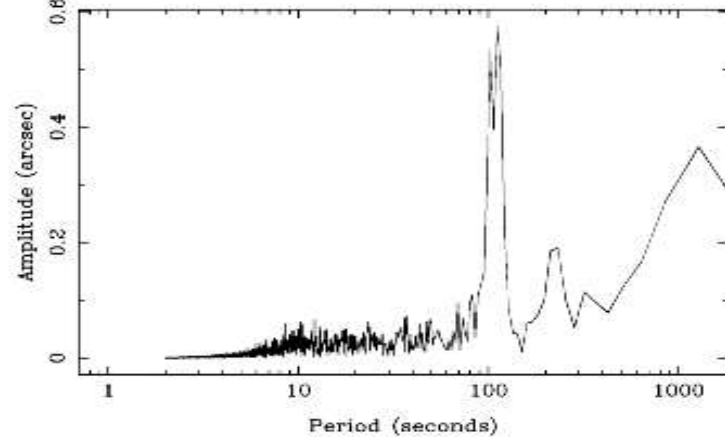
Figure 4: Tracking with nearly constant and equal elevation and azimuth velocities.
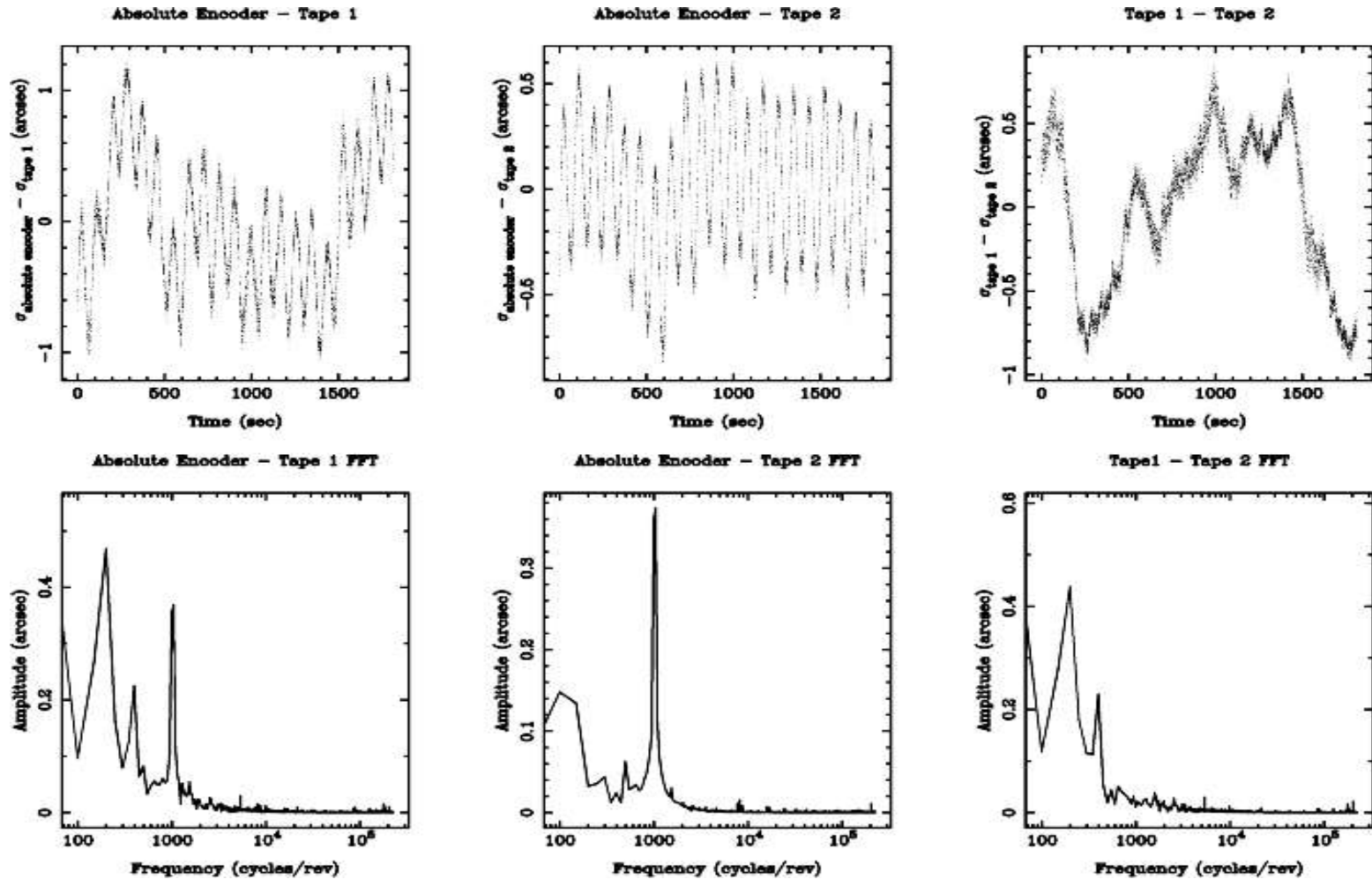
Figure 5: Results of a test where the telescope was commanded to run at a constant elevation velocity of 0.004 degrees/sec. "Absolute Encoder" refers to the Inductosyn while "Tape 1" and "Tape 2" refer to the tape encoders recently installed on the elevation drive arcs. The test was performed with the outer loop open so that all three encoders provide fully independent position measurements.

Figure 6: Results of a test where the telescope was commanded to run at a constant velocity with the outer servo loop closed. The data shown are for the Inductosyn encoders only.

Aluminizing

Construction is underway on an instrument enclosure that will contain almost all of the electronics necessary for aluminizing. Components were detailed and submitted for fabrication in October.

Another HP 34970A DAU was ordered specifically for gathering the volumes of data generated during aluminizing. It will be available to general facility at other times.
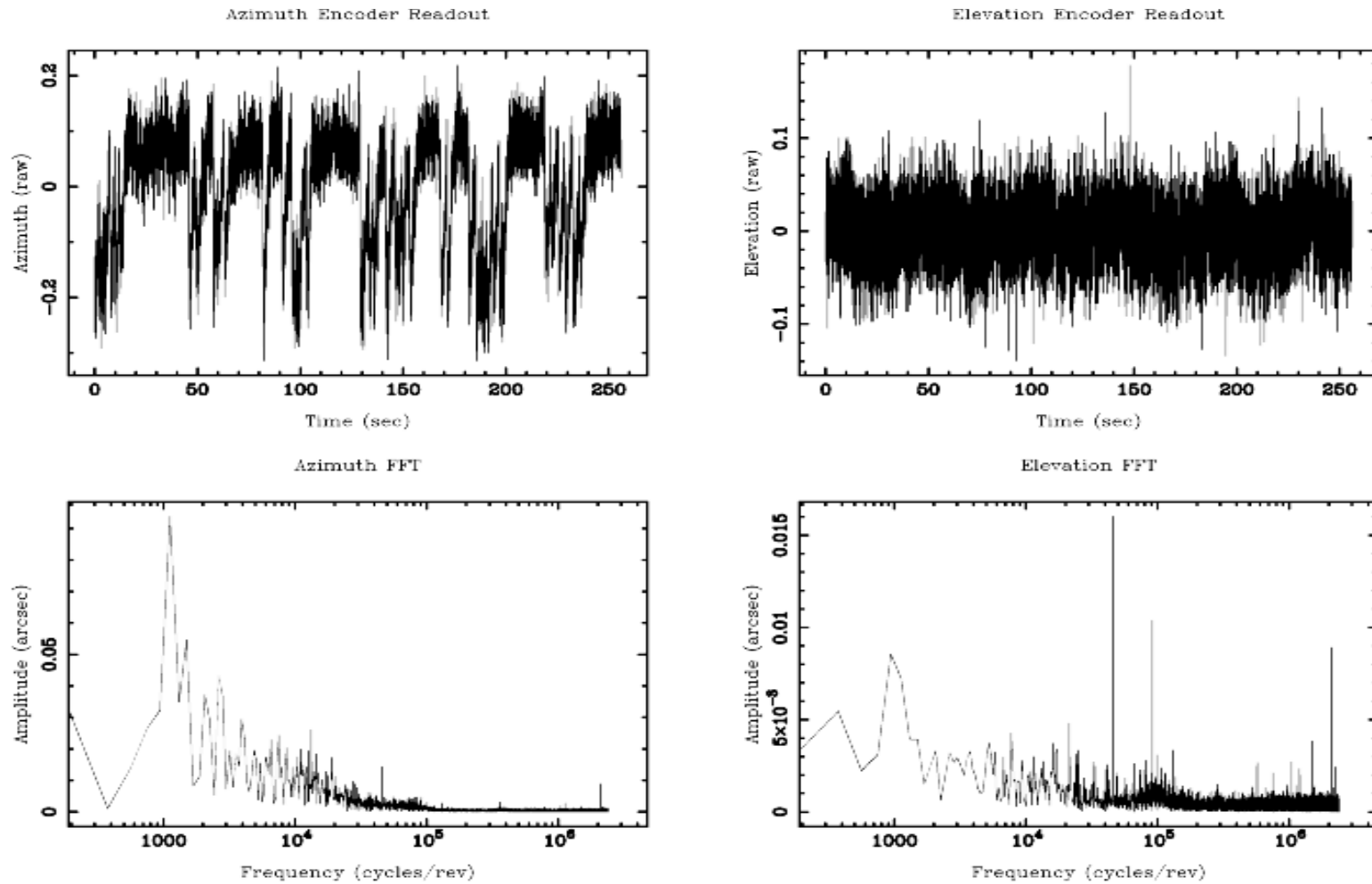
F/9 Topbox Shack-Hartmann Wavefront Sensor

The f/9 wavefront sensor was used during parts of eight nights during this reporting period. In addition to obtaining excellent "closed-loop" results, the open-loop telescope performance has been significantly enhanced by characterizing and eliminating the repeatable errors. Only instruments that utilize the f/9 topbox can access the full benefit of this wavefront sensor. Instruments that do not use the f/9 topbox can only remove the repeatable errors (open-loop).

Although we cannot monitor the off-axis wavefront continuously (due to limitations of re-using the old topbox, which was designed for a very small field), we can briefly interrupt the observations of the science instrument to perform on-axis wavefront sensing for correction of mirror figure, collimation, and focus. A flip-mirror temporarily re-directs the beam to the wavefront sensor. Figure 7 shows the results of measuring the wavefront and then correcting mirror figure and collimation on six separate nights.
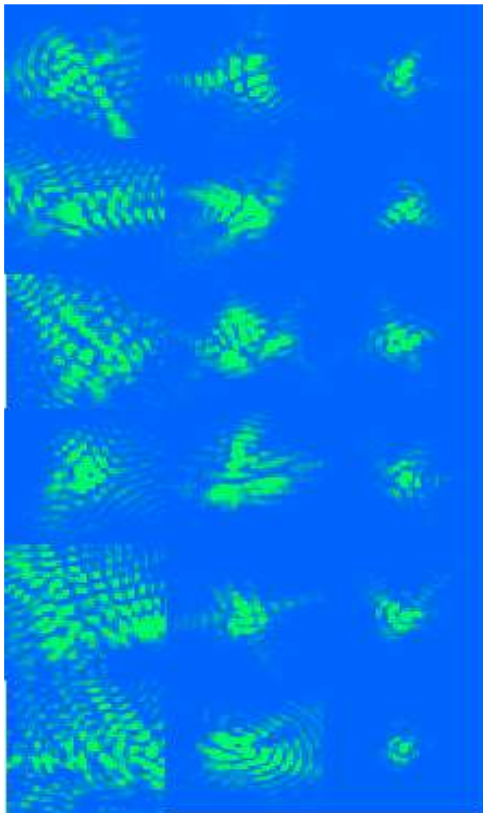
Figure 7: A series of images illustrate the improvements gained with the f/9 Shack-Hartmann wavefront sensor. Each row shows a series of three diffraction images calculated from the aberrations measured with the wavefront sensor. The first column shows the starting image psf shortly after opening the telescope each night. The second column shows the image psf after one correction of collimation and primary mirror bending. The last column shows the image psf obtained after a second correction of collimation and mirror bending. Each image shows the lowest 25% of intensity in a 0.5 x 0.5 arcsec box. The images are calculated from 19 Zernike modes (excluding tilt and defocus) measured from 90 sec of integration on a star. Two corrections produce a telescope diffraction image that fits entirely in a 0.1 to 0.2 arcsec box.

Ever since the primary mirror was delivered from the Steward Mirror Lab, we have operated with a baseline axial force optimization determined at zenith pointing with their lab interferometer. We took an opportunity to measure the mirror figure during operation with and without this force optimization. The only significant effect we could measure with our Shack-Hartmann was a change in third-order astigmatism shown in Figure 8.
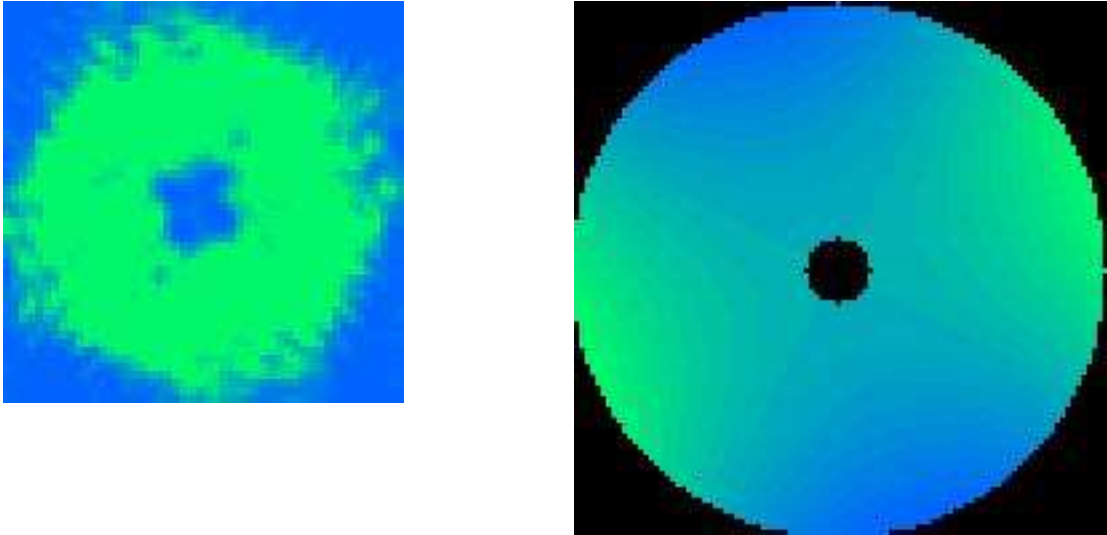
Figure 8: The contribution of image psf and pupil aberration (right) that is corrected with the force optimization determined at the Mirror Lab (north up, and east to right). This optimization has been successfully correcting a 1.7-micron amplitude error of third-order wavefront astigmatism.

Analyzing the wavefront aberrations measured prior to any mirror figure corrections reveals a set of stable repeatable aberrations that can be removed (in addition to the Mirror Lab optimization shown in Figure 8). These new errors include contributions from the f/9 secondary mirror and are shown in Figure 9.
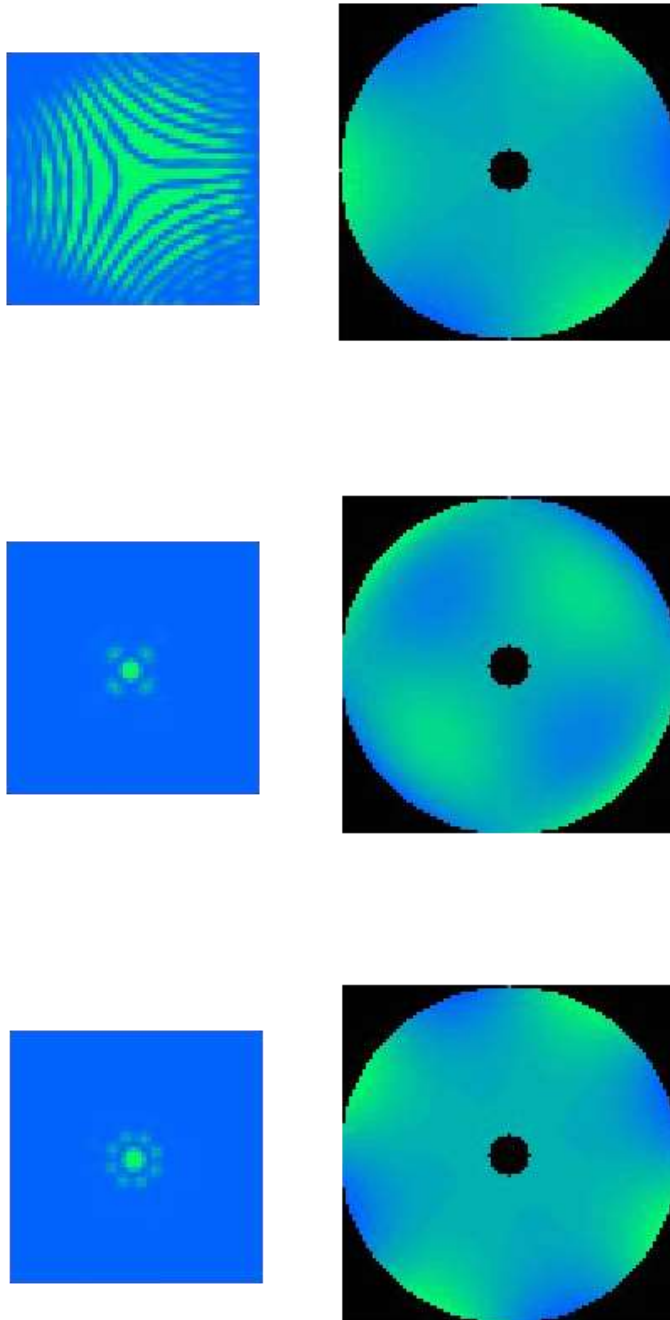
Figure 9: Three f/9 wavefront aberrations that repeat. The psf's (left column in 0.5 arcsec boxes) and pupil aberrations corresponding to these three modes are shown (north up and east right).

The large trefoil error has a wavefront amplitude of 1.2 microns, and the pupil image shows it is phased to the secondary mirror axial hardpoints, so it is likely due to the secondary mirror system. The two other repeatable aberrations are fifth-order astigmatism and 4-theta at 290 nm and 250 nm wavefront amplitudes, respectively.

Figure 10 shows typical image psf's before and after the removal of the three repeatable aberrations shown in Figure 9. Since these modes are repeatable, they can be removed even without access to the wavefront sensor. These psf's do not include defocus or third-order coma and astigmatism. The amount of residual astigmatism greatly depends upon the thermal state of the mirror and can be over 1 micron at the start of the night. The wavefront sensor is required to remove the astigmatism and any other non-repeatable errors.
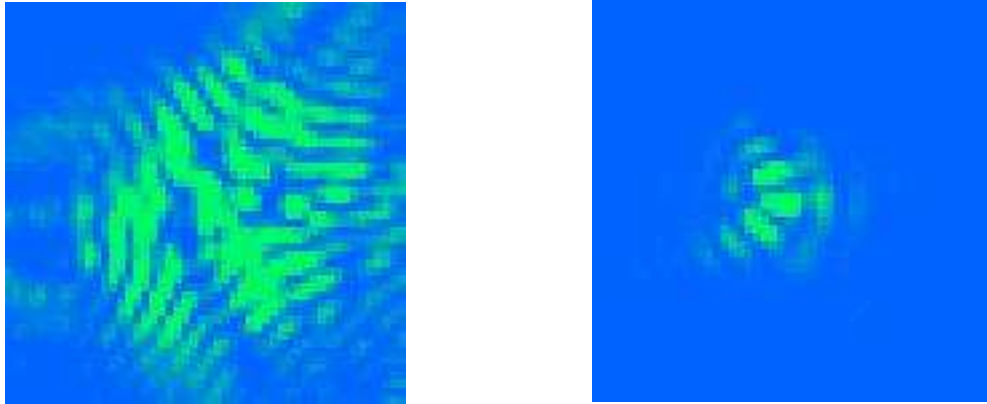

Figure 10: Diffraction images (calculated from measured wavefront errors) before (left) and after the removal of the three repeatable bending errors shown in Figure 9. This open-loop correction is now applied each time the primary mirror is lifted independent of the wavefront sensor. Third-order astigmatism is not shown in these images since it greatly depends upon the thermal state of the mirror, so the image at right is only realized without the wavefront sensor if the mirrors are in good thermal equilibrium with the ambient temperature. Otherwise, the wavefront sensor is required to remove the non-repeatable errors such as astigmatism.

On several nights, coma and defocus were measured as a function of elevation. The repeatable errors were built into an open-loop elevation correction tool (shown in Figure 11).
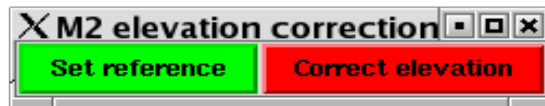
Figure 11: Simple GUI for correction of elevation-dependent coma and focus for the f/9 focus.

The correction helps the telescope operator by providing quick first-order focus and coma corrections vs. elevation for the f/9 focus. If the wavefront sensor is present, the errors can be further refined. The corrections are applied as differential adjustments to the position of the secondary. That way, they don't destroy any user-defined setups. Figure 12 shows the polynomial corrections and the residual errors as measured by the wavefront sensor. Clearly, further refinement of focus is required for imaging instruments, but the correction is adequate for spectrograph users.
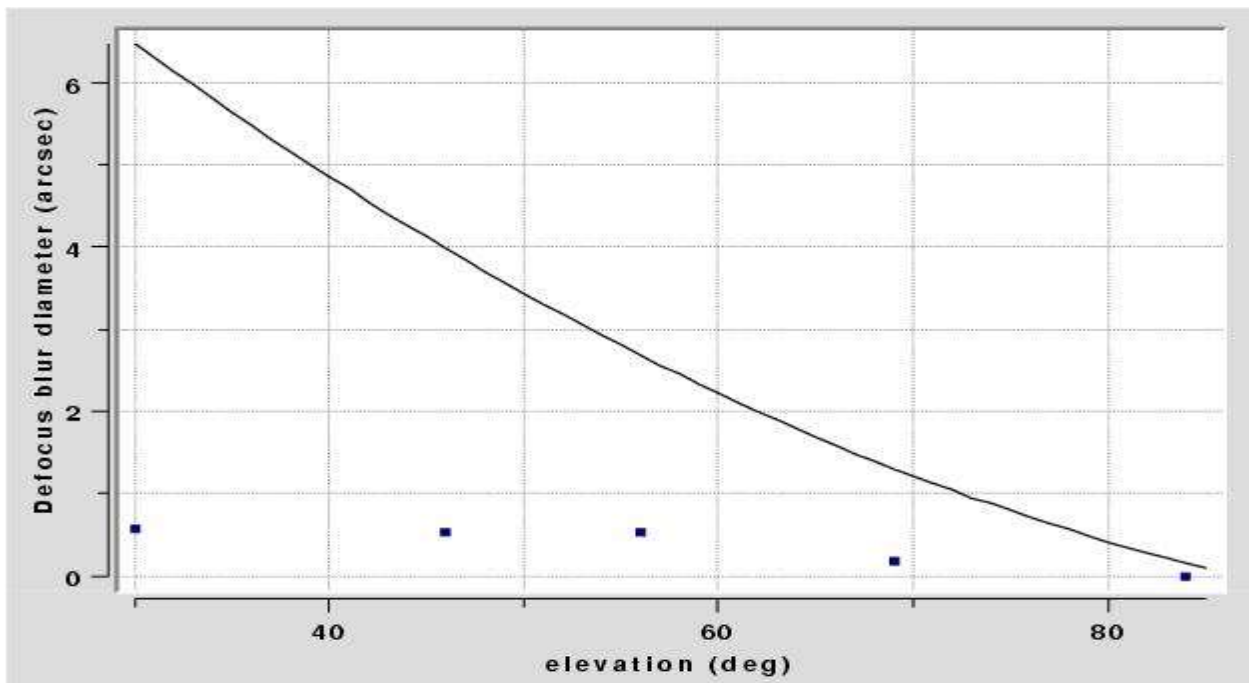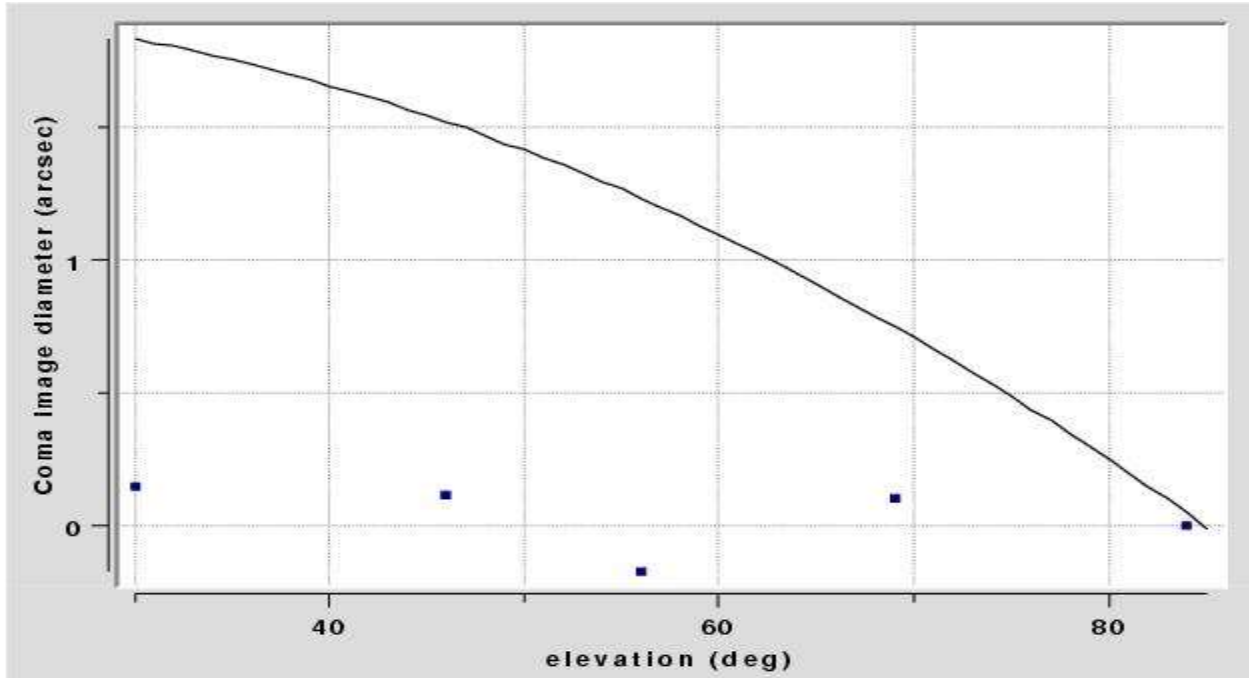
Figure 12: Polynomial corrections (solid lines) for elevation dependent coma (top) and defocus. After applying these corrections with the tool shown in Figure 11, the residual errors (squares) were measured with the wavefront sensor. Coma is corrected to about 0.1 arcsec, but the focus correction still needs improvement. The polynomials correct for 6-arcsec of focus blur and 2-arcsec of coma spanning elevations from 85 to 30 degrees.

A design was finalized for a topbox alignment laser. It will produce, with minimal setup and tweaking, a bi-directional 1 mm (<1 mrad divergence) beam coincident with the instrument rotator axis. This is needed principally for precision alignment of topbox optics and is also useful for auto-collimating the Cassegrain secondary. Parts will be fabricated in November.

F/5 Instrumentation

Components for the two bench spectrographs, Hectochelle and Hectospec, arrived safely at the FLWO basecamp on August 28. The two optical benches for the instruments were installed during the second week of September. This required the temporary removal of part of the rear wall of the spectrograph room on the third floor. The benches and a few of the larger optical components were lifted by crane through the opening into the building. Approximately 30 crates of spectrograph equipment were transported from the basecamp to the summit during the week following the installation of the benches. As the boxes arrived, a rough alignment of the equipment began.

In late September SAO engineers and technicians were on site to cable up the electronics, float the benches, network the computers, and test various motorized stages. During this period the two CCD dewars were pumped and filled with liquid nitrogen. The CCDs were tested to confirm that they were operating properly following shipping. Some tests were conducted to locate stray light within the spectrograph room. The liquid nitrogen lines, which run from storage vessels on the fourth floor through the ceiling of the spectrograph room, were installed and the auto-filler system was tested. The pressure in the storage vessels was found to be too high and therefore new pressure relief valves will be installed.

Installation and testing of the calibration lamps and calibration fibers was performed in early October. Work is also underway on the installation of the molecular iodine vapor absorption cell. This is a component of the instrument that will allow very precise wavelength calibration.

Detailed alignment of spectrographs, led by A. Szentgyorgyi and N. Caldwell, began in early October. Hectospec is nearly aligned and final alignment of Hectochelle will be completed in early January.

F/5 Mirror Support

Characterization and tweaking of the prototype mirror support electronics were done during the reporting period, with encouraging results on the support stiffness. The test gauge plug (which has a 0.005" clearance) fits snugly at all angles of the supported dummy mirror. There was a red herring discovered that resulted from a measured deflection of the edges of the dummy mirror that appeared to be a rigid-body motion of the dummy mirror along the gravity vector. Additional care-ful dial gauge measurements concluded that this was the "dishing" effect of the mirror's counter-weight on the dummy mirror plate. The good news on finding this behavior was that it caused us to completely evaluate the force/displacement behavior of all the tangent rod and hardpoint mechanisms. This data collection led to some minor shimming of the spring arrangement in the breakaways, so we move forward with a high level of confidence in the behavior of the breakaways in the hardpoints and tangent rods.

Minor changes to the circuit design on the mirror support card were found to be necessary during testing; these changes have been annotated to a new set of drawings used to produce a printed-

circuit version of the electronics. We expect to have a printed circuit in hand for testing during the next reporting period.

We also discovered that the control valves exhibited some odd behavior; only one of the two output connections on the valve body would go to 0 psi out. And, of course, the mirror cell was plumbed with the opposite output, which can only achieve about 0.5 psi at a minimum. This gave an erroneous force on the actuators at the zenith and horizon locations, where one wants 0 psi on either the lateral supports or axial supports, respectively. Reversing the plumbing connections solved this problem. Checking the part numbers of the valves during this process revealed that they had been ordered with nitrile seals, which do not last on the summit due to ozone contamination. They were returned to the vendor for seal replacement (with fluorocarbon) and will be re-installed prior to testing at SOML.

F/5 Hexapod

The design of a new amplifier and controller for the f/5 hexapod was started during the reporting period to replace the previous approach of a PC-controlled servo loop which used a serial link to command PWM amplifiers. The old design has been abandoned in favor of one using linear power amplifiers and an analog control loop that gets position and target data from a set of DACs updated by a microprocessor. The processor in the f/5 mirror cell reports the current hexapod lvdt values over a serial link to a control microprocessor, which in turn updates the position DACs at 100 Hz. The position DAC outputs are processed in an analog servo loop with a command DAC run by the system control PC over a second serial link. Control of the amplifier enables, motor brakes, and sensing limit switch status is also handled by this serial connection. We expect to have the new hardware built and tested during the next reporting period.

F/5 Baffles

N. Caldwell completed the f/5 baffle optical design. He and S. Callahan were then able to complete the tolerance analysis. S. Callahan and C. O'Neal then began designing the interfaces of the three baffles to the telescope. C. O'Neal is prototyping a rotary locking assembly to safely support the lower baffle next to the primary mirror. S. Callahan created a finite element model of the mid baffle to optimize the support and to determine the correct preloading of the support spider. R. James has begun the design of the upper baffle attachment to the f/5 support hub.

F/5 Test Tower Preparation

In preparation for testing the f/5 mirror cell on the Mirror Lab interferometer, R. James and S. Callahan designed six new attachments to the f/5 cell. These attachments allow six azimuthal rotations of the cell above the test tower at the correct height.

Secondary Hub Coolant Manifolds

C. Wainwright, R. James, and S. Callahan worked with the mechanical design team to detail a new secondary coolant delivery layout. This design minimizes the obscuration of the telescope while providing adequate coolant to supply all three secondaries.

Computers and Software

Data Server

The new data server has been running continuously for most of September and October. During this period, several new threads were added and additional functionality was added to existing threads.

A RainWise thread was added to the data server that allows extensive weather information to be obtained from the RainWise remote weather station. These weather data include barometric pressure, temperature, wind chill, relative humidity, as well as wind direction and speed. These data are used to derive a dew point, which is critical in preventing condensation on the primary mirror and in recognizing potential icing on heat exchangers.

Two new threads were added to monitor T-series thermocouple data from the primary mirror. Although these thermocouples are not as numerous as the E-series, the T-series thermocouples are insulated, unlike the E-series. It is believed that the T-series thermocouples would more accurately reflect the true glass temperature.

A data server thread monitor GUI was completed. This GUI reports the current status of the following threads within the data server: AO Neslab, Carrier, Cell, F9 Secondary, Logger, Mount, NE Cell HP DAU, NW Cell HP DAU, Pit Neslab, Pit HP DAU, RainWise, SE Cell HP DAU, Shop HP DAU, SocketServer, SW Cell HP DAU, and Vaisala. Thread status is indicated both by a label (i.e., "Running") and by a status color (e.g., green for no errors).

An f/9 secondary thread was activated that uses a Tcl script to read all hexapod-related data into the data server. This Tcl script will be replaced with a Ruby class.

Functionality was added to the logger class so that a spreadsheet is produced of all data within the data server every hour, 24 hours per day, at 5 minutes before the hour. These spreadsheets can be viewed at the following URL: http://hacksaw.mmto.arizona.edu/~mmtop/Logs/

The spreadsheet is divided into the following sheets: 1) Carrier, 2) Cell, 3) Pit Neslab, 4) Pit HP DAU, 5) Mount, 6) Shop HP DAU, 7) Vaisala, 8) RainWise, 9) NE Cell HP DAU, 10) SW Cell HP DAU, and 11) F9 Secondary. These spreadsheets have already proved to be very useful for analyzing and plotting telescope system data.

Network Protocols

For a number of years, a simple ASCII message protocol has been used at the MMT for communication between the various telescope control subsystems and the operator GUIs. During this period, the protocol was enhanced and generalized. Revisions affected the mount, hexapod, and cell control subsystems. We have learned that within our local network the cost to send messages is constant, and essentially independent of packet size (at least for the relatively small messages that we commonly send). The protocol has been modified to take this behavior into account, and now makes it possible to send large bundles of information in single packets when possible.

Miscellaneous

Ruby code was written for a msg server for the current FOCUS msg server. This msg server is one method to control the hexapod. The msg protocol is used extensively by SAO staff. Previously, the msg protocol had been available only in Tcl and C. Having similar code available in Ruby allows msg communication with scripts written in Ruby.

A revised version of the telstat GUI, which displays a summary of telescope status information for the operators and observers, was written that uses the new "all" command available for the mount crate. Use of this command reduces the socket communication load on the mount crate.

A new, simplified f/9 hexapod GUI was created that will use an ASCII protocol from the hexapod crate. Plans are underway to move much of the code that is currently in Tcl into the VxWorks code within the hexapod crate. This should improve hexapod performance and simplify future code development.

A new f/5 hexapod GUI was created, similar to the f/9 GUI just described, that will communicate via an ASCII protocol with the new f/5 controller when the firmware for the f/5 is finalized. An f/5 cell GUI was created that will also communicate with the f/5 controller through an ASCII protocol.

Optics

No activity to report.

General Facility

The cables going up the OSS to the secondary have been reinstalled into cable trays that are securely attached to the structure. Room has been allocated in the same trays for the f/15 cables. The cabling along the spider has been adjusted to minimize its cross section; additional work is planned to refine this.

Cabling has been installed from the 26V rack to the drive room in order to provide computer control of the blower via the fiber interface. This task needs to be completed and tested before removing the old manual control.

The new secondary hoist safety switch is adjusted but needs to be connected to the 26V system. We also need to develop physical stops to prevent the trolley from cocking when it hits the limit switch. Currently, it can over-travel and go beyond the limit.

New cables were run from the Cyclades to each of the four corners of the cell to provide access to DAUs for thermal measurements of the cell. An additional DAU was installed at the southwest corner.

At the request of SI safety people, the desiccant oven was moved out of the Summit Support communication room to a safer location.

Maintenance and Repair

An issue of recent concern has been an intermittent problem with the building drive. Symptoms began in September and culminated in the return of one of the Copley drive amplifiers to the factory for repair. The initial problem began with infrequent building collisions with the telescope, which occurred under both slewing and tracking operation. During the early stages of troubleshooting, damage occurred to one of the Copley amplifiers. This damage is believed to have been caused by a foreign object (a paper clip) which had been lodged inside for many years and was jarred loose by movement. This unit was returned to the factory for repairs and has been reinstalled. During the repair period an attempt was made to run the telescope on one drive by overriding the "minor fault" and reducing the building velocity. Tracking was possible but at too great a reduced velocity to be useful for effective operation. Also during the repair period, building drive spare electronics cards were located, repaired, and updated to the latest revision.

When the repaired Copley was reinstalled, spares were functionally tested to the level of our present system knowledge. We have requested and are anticipating some test specifications from the system designer (K. Harrar) to further refine the test processes and procedures. Presently the building drive is operating but we have not clearly identified a specific cause of the failure, nor have we positively identified what has allowed our current operational ability. One likely cause is an intermittent "minor fault." We are monitoring the situation closely. The "repair" of the building drive system required a large amount of time and effort to organize and fully understand its operation. Two tangible results of this effort were K. Van Horn's complete overhauling of the documentation, and B. Comisso's and C. Knop's repairing, building, testing, and revising spare electronics.

The video camera system for the chamber was resurrected, repaired, and installed. It works reasonably well with the floodlights on, less well with its own IR illuminators and the incandescent lights, and not at all in darkness. In addition, the IR does create problems with the instruments. It appears to be a good system for monitoring activity in the observing chamber during the day but will not be used during observing.

Visitors

September 7: Peter Vekinis (Vekinis Consulting, Luxembourg) visited the MMT to gather ideas for an MMT brochure he is producing.

September 19: Dr. Fumihide Iwamuro (Associate Professor of Astronomy, Kyoto University, Japan) and Dr. Yoshida (general manager of Okayama Astronomical Observatory, Japan), accompanied by C. Foltz.

October 17: A group of high level engineers and physicists involved in military application of long range optical systems (laser ranging and imaging), accompanied by P. Wehinger (SO). Included in this group are Dennis Fisher (Optical Engineer, Vandenberg AFB), Hector Gurrola (White Sands

Missile Range), Randy Dewees and Mike Lovern (US Navy), Dr. Juergen Pohlmann (Director, Science Programs, Department of Defense, Missile Defense Agency, Advanced Systems Deputate, The Pentagon), Joe and Elizabeth Houston (Joe is a former SPIE President and VP for research with Itek, and is currently a consultant to the Defense Department on laser ranging and optical systems), Delmar Haddock (Space Warfare Systems Center, San Diego), George Norwood and Michael Lowen (New Mexico Technology Group, Software Engineers, Optics Dept., White Sands Missile Range). While on site, A. Szentgyorgyi provided some explanation of the Hectospec and Hectochelle.

Publications

MMTO Internal Technical Memoranda

None

MMTO Technical Memoranda

None

MMTO Technical Reports

None

Scientific Publications

02-11   The Nascent Bipolar Nebula Surrounding the Carbon-Rich Variable CIT 6: Transition to Axisymmetry
Schmidt, G. D., Hines, D. C., Swift, S.
ApJ, **576**, 429

02-12   Wolf-Rayets in IC10: Probing the Nearest Starburst
Massey, P., Holmes, S.
ApJ Letters, in press

02-13   Progress of the MMT Adaptive Optics Program
Wildi, F. P., Brusa, G., Riccardi, A., Allen, R. G., Lloyd-Hart, M., Miller. D., Martin, B., Biasi, R., Gallieni, D.
SPIE, **4494**, 11

02-14   The Spectroscopic Variability of GRB 021004
Matheson, T., Garnavich, P. M., Foltz, C., West, S., Williams, G., Falco, E., Calkins, M. L., Castander F. J., Gawiser, E., Jha, S., Bersier, D., Stanek, K. Z.
Submitted to *ApJ Letters*

02-15   AAS Annual Report

Foltz, C. B.
BAAS, **35**

Observing Reports

Copies of these publications are available from the MMTO office. We remind MMT observers to submit observing reports, as well as preprints of publications based on MMT research, to the MMTO office. Such publications should have the standard MMTO credit line: "Observations reported here were obtained at the MMT Observatory, a facility operated jointly by the Smithsonian Institution and the University of Arizona."

Submit observing reports and publication preprints to *bruss@mmto.org* or to the following address:

MMT Observatory
P.O. Box 210065
University of Arizona
Tucson, AZ 85721-0065

MMTO in the Media

No activity to report.

MMTO Home Page

The MMTO maintains a World Wide Web site (the MMT Home Page) which includes a diverse set of information about the MMT and its use. Documents that are linked to include:

1. General information about the MMT and Mt. Hopkins.

2. Telescope schedule.

3. User documentation, including instrument manuals, detector specifications, and observer's almanac.

4. A photo gallery of the Conversion Project as well as specifications and mechanical drawings related to the Conversion.

5. Information for visiting astronomers, including maps to the site and observing time request forms.

6. The MMTO staff directory.

The page can be accessed in two ways. First, it can be loaded via URL *http://www.mmto.org*. Second, it can be accessed via a link from the OIR's MMT page at URL *http://cfa-www/cfa/oir/MMT/mmt/foltz/mmt.html*.